A billiard calculation of the dynamical friction of an Atomic Force Microscope

William Mather*
School of Physics
Georgia Institute of Technology,
Atlanta, GA 30332-0430, U.S.A
(Dated: August 23, 2007)

We model the "dynamical-mode" of function, defined as a mode conceptually between contact modes and tapping modes, for an atomic force microcope (AFM), using as a model a two-dimensional impact oscillator moving across a sinusoidal surface at constant horizontal velocity on average. General predictions and numerical observations are given, with comments on the difficulties in determining symbolic dyanmics.

PACS numbers: PACS!
Keywords: impact oscillator, chaotic, periodic orbit theory, atomic force microscope, AFM, billiards, tribology

Georgia Tech PHYS 7224:
CHAOS, AND WHAT TO DO ABOUT IT
course project, spring semester 2005
advisors: R. Paškauskas, P. Cvitanović.

I. INTRODUCTION

Resting on the edge between classical and quantal, the atomic force microscope (AFM) [2] provides an immensely useful link for experimental determination of the height profile and certain physical properties of a nanoscale surface. The basic device consists of a cantilever with a finely constructed tip, which interacts with the surface with a precision determined by the quality of the tip. Through various methods of transverse and longitudinal motion, the tip is deflected by the surface in a measurable manner, typically through the deflection of a laser beam onto a photodiode detector array (typically a set of 2 or 4, where intensities are compared for measurements).

Three primary modes of operation are used in the laboratory: 1) contact, 2) non-contact, and 3) "tapping" or dynamical mode. The first two are the most traditional, probing through the use of dragging as in a record needle, and indirect van der Waals forces, respectively. The third choice uses a more complicated and less well-defined alternative of allowing the tip to neither remain on the surface nor to remain completely off.

This dyanmical mode has practical advantages over the first two in that direct contact is brief, avoiding damage to the surface and tip due to static frictional effects, but the tip-surface coupling remains strong in a measurable sense. One such measurement that could be useful in various disciplines for surface imaging is the kinetic friction, defined as:

$$\langle f \rangle = \lim_{\Delta x \to \infty} W/\Delta x \tag{1}$$

where W is the average work needed to pull the tip across the surface over a distance Δx. We may take Δx in the above formula to equal asymptotically the run-time multiplied by the drag velocity v_0, since the cantilever should in long times move approximately the same distance as its tip. We will argue later in this paper that resonances in this observable arise due to periodicity of the surface.

Regular mica surfaces provide a clean testing ground for various AFM techniques, in which context contact mode theories have been presented [5]. We seek to explore the dynamical regime of operation on this nearly sinusoidal surface through the technology presented in [4]. Through ideas presented in [3], we might begin to develop a theory for sliding friction in general.

II. PRELIMINARY: MAPPING / REFLECTION JACOBIANS IN FLOWS

This section is included to justify a reflection Jacobian that is referenced later in this paper, and may be skipped if one wishes. In addition, my advisors for this project expressed that some confusion may be still lingering in the literature for the general treatment of such Jacobians, and so there is little harm in refreshing what should be known.

For continuous flows, computation of the Jacobian results from the ODE, $\dot{\mathbb{J}} = \mathbb{A}\mathbb{J}$, where $\mathbb{A}$ is the local stretching matrix. Flows that encounter discontinuous maps in phase space cannot be treated in this same way, but we can many times neatly separate the smooth and non-smooth contributions of the Jacobian through a straightforward procedure of neighborhood manipulation. A brief summary of this process is given in the remainder of this section, and I've been told a similar derivation can be found in Gaspard's book.

*Electronic address: gte994m@prism.gatech.edu

We assume that the discontinuous, but instantaneous, map has domain and range on some surface that satisfies the surface equation $F(\vec{x}) = 0$. For billiards, this surface is typically visualized as purely spatial, but in fact, it cuts through velocity space in a way that defines reflections. On this surface, we define the map as R. We begin and end with a small neighborhood that is infinitesimally away from the surface in question.

Motivated by the fact that the map preserves time under mapping, we project neighborhoods onto the surface and keep track of the small time differences, inherent in projection, in some new coordinate δt, while the surface tangent coordinates of intersection can be given as $\delta x_\perp$. δt is unaffected by the map, thus the stretching due to the map portion is purely in tangential coordinates (as expected). We have kept track of δt and can then reproject *off* of the surface after mapping, and return to a neighborhood defined back in full phase space at a given sharp value of time. Returning all points to the same time in the end is critical, or else our usual notion of a continuous flow Jacobian is not satisfied.

We do precisely this through the following operations:

$$\mathbb{P} : \begin{array}{c} \delta x_\perp = \delta x + v(x)\delta t \\ \delta t = -\frac{\nabla F \cdot dx}{\nabla F \cdot v} \end{array} \tag{2}$$

$$\mathbb{P}^{-1} : \delta x = \delta x_\perp - v(x)\delta t \tag{3}$$

... and the map Jacobian in perpendicular coordinates:

$$\left(\frac{\partial R}{\partial x_\perp}\right)_{i,j} = \frac{\partial R_i(x)}{\partial x_{j,\perp}} \tag{4}$$

Combining all the operations, we get the full Jacobian for the map portion (which is manifestly *different* from any Jacobian that considers $\frac{\partial R}{\partial x_\perp}$ alone):

$$\mathbb{J}_{map} = \mathbb{P}^{-1} \cdot \frac{\partial R}{\partial x_\perp} \cdot \mathbb{P} \tag{5}$$

Notable terms found in damped billiards under acceleration can be found as arising from the above. Curvature terms derive from $\frac{\partial R}{\partial x_\perp}$, due to differentiation of surface normals. Reduction in normal velocity neighborhood width by γ also derives from $\frac{\partial R}{\partial x_\perp}$, but reduction in the normal spatial neighborhood width is actually due to a mismatch in velocities in the two projections. Acceleration terms occur due to a similar mismatch in the two projections.

A diagram of the calculation is provided on an attached page at the end of the document.

III. MODEL

We investigate this system through the use of a two-dimensional impact oscillator, a rich system that is well studied in the the case of one-dimension and is believed to possess windows of chaotic behavior for certain parameter values [6–8]. The idea is to mimic an oscillating tip pressed against the surface, which is kept active by the translational motion of the cantilever.

The model is a harmonic oscillator, with horizontal frequency ω_h and vertical frequency ω_v, with its harmonic center point moving horizontally with constant velocity v_0. The non-linearity enters through damped reflections off a sinusoidal surface of given period and amplitude. So that the tip does not relax into an oscialltion that potentially never intersects this surface, the vertical component of the harmonic center is assumed to be below the maximum of the surface (no hovering).

At each impact, the velocity is assumed to reflect with law given by Eq. 11 in the next section, but the restitution coefficient γ is made to go into the elastic limit $\gamma = 1$ for low impacts, specifically in a linear manner proportional to normal velocity below some cutoff. The motivation is that while physically we do not expect nearly grazing impacts to prevent an AFM tip from crossing a surface maximum, "chattering" [6] can lead a particle to stick to a surface in finite time through a cascade of bounces. We do not care to model sliding dyanmics or bother analytically following through infinite bounces, so we circumvent this problem instead.

One goal is to compute the mean kinetic friction, defined above. The harmonic part of the trajectory conserves energy, so all the work expended to pull the tip a given distance in this model resides in the inelastic collisions. In prinicple, the technique of periodic orbit expansions [4] might find this coefficient for arbitrary parameter values with high precision, though in practice, we are limited my our understanding of the symbolic dyanmics and by the existance of periodic orbits as the only periodic structures.

The formula connecting the dyanmics of our system to the kinetic friction derives from understanding all energy loss is due to contact forces alone. Letting ΔE_k be the energy lost in a particular impact on a given trajectory $\mathbf{Q}$, the mean measured friction is for long trajectories:

$$f_{\mathbf{Q}} = \lim_{N\to\infty} \frac{\sum_{k=1}^{N} \Delta E_k}{v_0 t_N} = \frac{1}{v_0} \lim_{N\to\infty} \frac{\sum_{k=1}^{N} \Delta E_k}{\sum_{k=1}^{N} \Delta t_k} \tag{6}$$

... with t_k the total elapsed time from start to impact k.

We expect that the dividend and the quotient become essentially statistically independent Gaussian variables in the long time limit, and so our average over the natural measure should factor:

$$\langle f \rangle = \frac{\langle \Delta E \rangle}{v_0 \langle \Delta t \rangle} \tag{7}$$

We can compute the averages of ΔE, Δt directly using periodic orbit theory.

It will conveniant, due to scaling relations, to instead define an observable: which we will refer to as the friction

coefficient:

$$K_f \equiv f/v_0 = \frac{\langle \Delta E \rangle}{v_0^2 \langle \Delta t \rangle} \tag{8}$$

IV. EQUATIONS OF MOTION

Though trivial considered independently, the equations of motion when free are for each coordinate (given for simplicity now in the comoving frame of the harmonic center):

$$\begin{bmatrix} x_i' \\ v_i' \end{bmatrix}_c = \begin{bmatrix} \cos(\omega_i \Delta t) & \frac{1}{\omega_i}\sin(\omega_i \Delta t) \\ -\omega_i \sin(\omega_i \Delta t) & \cos(\omega_i \Delta t) \end{bmatrix} \begin{bmatrix} x_i \\ v_i \end{bmatrix}_c \tag{9}$$

. . . for i being the horizontal and vertical directions. Since the system in the comoving frame is due to a constant matrix, the Jacobian, $\mathbb{J}_t$, in the comoving frame is identical to the matrix above. To translate to "fixed" coordinates, we can use the equation:

$$\begin{bmatrix} x_i' \\ v_i' \end{bmatrix} = \mathbb{J}_t \begin{bmatrix} x_i - x_{0i} \\ v_i - v_{0i} \end{bmatrix} + \begin{bmatrix} x_{0i} + v_{0i}\,\Delta t \\ v_{0i} \end{bmatrix} \tag{10}$$

. . . with $v_{0i} = 0$ for $i =$ vertical (zero vertical dragging velocity) and $\vec{x}_0$ is the initial position of the harmonic center. We see explicitly that the Jacobian in the comoving frame is equal to the Jacobian in the non-deflected segments of the trajectory (just as with the totally free system). Thus the eigenvectors of the Jacobian are the eigenvectors of the original matrix, leading us to complex pair eigenvalues $\lambda_i(t) = e^{\pm i\omega_i \Delta t}$ for i both components. Notice there is no coupling between components yet.

The reflection from velocity $\vec{v}$ into $\vec{v}\,'$ is given for surface normal $\hat{n}$:

$$\vec{v}\,' = \vec{v} - (1+\gamma)\ \hat{n}(\hat{n}\cdot\vec{v}) \tag{11}$$

We can see that the tangential velocity to the surface and the surface spatial points themselves are unchanged under a reflection, to zeroth order. If $v_\parallel$ is tangential and $v_\perp$ is normal velocity to the surface, then the new velocities $v_\parallel'$, $v_\perp'$ are:

$$\begin{bmatrix} v_\parallel' \\ v_\perp' \end{bmatrix} = \begin{bmatrix} 1 & 0 \\ 0 & -\gamma \end{bmatrix} \begin{bmatrix} v_\parallel \\ v_\perp \end{bmatrix} \tag{12}$$

The Jacobian of the reflection is harder to compute than before, but the method presented earlier will do the trick. A local set of coordinates for a parallel and transverse directions makes the calculation relatively straightforward. The net result is ($v_\parallel$, $v_\perp$ are the incident velocity vectors, κ is the surface curvature, and $A_{0\perp}$ the normal component of acceleration in Cartesian local coordinates):

$$\begin{bmatrix} x_\parallel' \\ x_\perp' \\ v_\parallel' \\ v_\perp' \end{bmatrix} = \mathbb{J}_R \begin{bmatrix} x_\parallel \\ x_\perp \\ v_\parallel \\ v_\perp \end{bmatrix} \tag{13}$$

$$\mathbb{J}_R \equiv \begin{bmatrix} \mathbf{\Gamma} & \mathbf{0} \\ \mathbf{\Theta} & \mathbf{\Gamma} \end{bmatrix} \tag{14}$$

$$\mathbf{\Theta} \equiv \begin{bmatrix} \kappa(1+\gamma)v_{0\perp} & \kappa(1+\gamma)v_{0\parallel} \\ -\kappa(1+\gamma)v_{0\parallel} & -\frac{\kappa {v_{0\parallel}}^2 - A_{0\perp}}{v_{0\perp}}(1+\gamma) \end{bmatrix} \tag{15}$$

$$\mathbf{\Gamma} \equiv \begin{bmatrix} 1 & 0 \\ 0 & -\gamma \end{bmatrix} \tag{16}$$

. . . from which it can be read to have eigenvalues $1, 1, \gamma, \gamma$, and determinant γ^2. This Jacobian is rotated into the lab frame to get a Cartesian neighborhood. Numerical experiements on the above functional form of the Jacobian support all terms in the above matrix.

The one remaining aspect of the coordinates is the non-trivial dependence of the system (and the full 5-dimensional Jacobian) on the extension parameter, which is how far in the longitudinal direction the point of zero harmonic forcing rests leading or lagging from the particle. Though the absolute reference point of the harmonic center has simple linear time dependence, the relative extension defines a phase which is important for the particle, say, for phase locking. The components in the 5×5 Jacobian matrix cooresponding to this coordinate are simple, and only result from harmonic flight segments. Here the Jacobian components can be derived by inspection from the equation of motion Eq. 10.

Finally, a projection of the Jacobian matrix onto the Poincare surface (just the surface of the billiard system) can be done through a formula in ChaosBook [4] under "stability". Then, we can define a Jacobian matrix purely in the coordinates that neglect the height of the particle (determined by the function of the surface), and transform from starting neighborhoods (defined on the Poincare surface) to full phase space neighborhoods by the rule (δx_P identifies the change in x on the Poincare section, $\frac{df}{dx}$ is the derivative of the surface function):

$$\delta x_P \quad \longrightarrow \quad \delta x = \delta x_P, \quad \delta y = \frac{df}{dx}\delta x_P$$

We will in addition require that periodicity be inforced on the trajectories, such that the tip at one location is identified with itself translated one surface periodic length (as well as the harmonic center translated the same distance). The important non-periodic remnant of the system will be the relative extension of the particle from the harmonic center.

Again, we emphasize that trajectories which go into "contact" with the surface through a cascade of bounces are not included, due to the complexities involved. If we assume that such a cascade is carried through analytically after a certain point, we rigorously flatten part of the Jabobian matrix in the normal direction of the surface. Since expanding eigenvalues are the most important, we might continue to compute observables for this reduced phase space, but as stated, we avoid these complications.

V. PHYSICAL PARAMETERS OF THE MODEL

The physical parameters used in this problem mimic those of Tyson in an earlier project, also using the rest-point of the AFM tip precisely in the middle of the surface's maximum and minimum. The parameters should approximate the dimensions of an AFM tip on mica.

vertical angular frequency:
$\omega_{vertical} = 40x10^3$ rad/s
horizontal angular frequency:
$\omega_{horizontal} = 250x10^3$ rad/s
effective tip mass:
$m = 408x10^{-12}$ kg
lattice spacing:
$a = 0.52$ nm
surface amplitude:
$H = 0.05$ nm

VI. DIMENSIONAL AND SCALING ANALYSIS

Several dimensionless or (equivalently) natural parameters exist in the system and set the scale for observations that might be made in a laboratory. For typical values of γ, such as $\gamma \approx 0.7$, these parameters predict most of the general behavior of the system.

Firstly, we notice that γ can change the dyanmics of the system quite dramatically. The limits $\gamma \to 0, 1$ are both singular in a sense. $\gamma \to 0$ causes all impacts with acceleration pointed into the surface to stick until acceleration reverses direction, which may never happen in this model after such an impact. Additionally, contact sliding dynamics should become the most important in this regime, as compared to impact dynamics. $\gamma \to 1$ creates a conservative system, and with available phase space is not shrinking upon each impact, we are not even sure if the system is bounded!

Intermediate γ values should produce what we expect: low values tend towards low dimensional attractors, such as stable periodic orbits and chattering cascades, and higher values tend towards the inherent oscillatory behavior of the Hamiltonian free flights, such as chaotic attractors and even quasiperiodic orbits. For this reason, choosing a value $\gamma \approx 0.7 \approx \sqrt{0.5}$ (γ^2 occurs often is the reasoning here) for typical numerical investigations makes sense.

The first ratios of dimensionful parameters to notice relate the scale between horizontal and vertical times and lengths:

$$\begin{array}{rcl} \alpha^{-1} & \equiv & \omega_h/\omega_v \approx 6.3 \\ \epsilon^{-1} & \equiv & a/H \approx 10. \end{array} \tag{17}$$

$\frac{2\pi}{\omega_h}$ thus sets the shortest time scale, besides the assumed instantaneous impact time, in the dynamics, and we can expect this time should be (and is) our computational natural time for surface intersection searching and so forth.

We find, after convincing ourselves through simulations, that the most important time scale for the actual dyanmics is rather:

$$\tau \equiv \frac{2\pi}{\omega_v} \approx 0.16 \text{ ms} \tag{18}$$

We can imagine that the fast horizontal motion is entrained in the slow bouncing of the AFM tip. Physically, we should not expect significant horizontal stretching in the tip, so we are not surprised when we find numerically that horizontal displacements stay close, relatively, to their resting point.

The sliding velocity has a natural unit that derives from τ and a, with the idea that we should associate an integer when the periods of vertical bouncing and horizontal translation coincide. We define:

$$v_{0,natural} \equiv \frac{a}{\tau} \approx 3.3 \ \mu\text{m/s} \tag{19}$$

Additionally we define the sliding velocity in natural units:

$$\eta \equiv \frac{v_0}{v_{0,natural}} \tag{20}$$

η neatly organizes the nearly repeating patterns in observables as we increase sliding velocity. We will see that two different conditions for η will become important:

$\eta =$*odd integer, Low Friction / "Splashing"* :
Imagine first $\eta = 1$. Then, a full vertical oscillation should coincide with a surface period. Such behavior is precisely out of phase with hitting the peaks of the surface once per a given number of units cells having been traversed, and thus regular impacts should occur on the *lower pieces* of the surface, if the particle hits a contained region regularly at all. Given that we assumed the harmonic resting point is mid-surface, the particle deaccelerates typically before impact, and the energy loss should be less than hitting peaks. This argument should hold also for resting points located at heights still between surface extrema. "Splashing" will be explained shortly, but this descriptor relates to the much higher incidence of low-angle (and low energy loss) bounces per surface period for low-lying trajectories, and generally more problems with grazing impacts.

$\eta =$*even integer, High Friction / "Bouncing"* :
We can argue similarly that for these η, the dynamics corresponds to hitting only peaks. The dynamics in these regions typically is much cleaner, involving attractors such as periodic orbits, and impacts typically are closer to normal incidence that for odd η. This behavior can be considered as resonant absorption in the system, and these peaks might be robust in parameter space due to frequency locking effects, as long as the resonant condition is satisfied.

A few comments may be made on vertical velocities. Notice that if the surface were completely flat, then if we assume the resting point is at or below the surface, all vertical motion scales to zero asyptotically. Indeed, the only way coupling between horizontal motion (which we think of as delivering energy) and vertical motion can occur is due to surface normals with horizontal components. If we assume our surface is described by $y = \epsilon f(x)$, where epsilon is small, then the x-component of the surface normal is ($f'(x)$ is the first derivative of f):

$$n_x = \frac{-\epsilon f'}{\sqrt{1 + (\epsilon f')^2}} \approx -\epsilon f'(x), \quad |\epsilon f'(x)| \ll 1$$

... so since we think of our verical scale as small, the vertical velocity should depend in some simple linear way on the surface height, contributing only an order of magnitude of smallness between the vertical and horizontal velocities in our case.

The final quantity we investigate here is the friction coefficient. Since both components of velocity have good reason to be proportional to v_0, we expect each impact should lose on average $\Delta E \propto v_0^2$. In comparison, if we imagine the resonant modes hitting peaks only, the mean time for impact $\langle T \rangle$ should not change greatly with v_0 due to the assumed fixed frequency of vertical harmonic motion - ie., the size of the oscillation ideally does not change return time for large bounces (corrections due to surface height vanish for large bounces).

Hence, arguments lead us to:

$$f \propto \eta, \text{ at even } \eta$$

... which explains why the friction coefficient, as defined previously, is a sensible object to measure.

Accounting for the reduction of vertical velocity, and assuming that vertical velocity is the most important component for energy absorption, it makes sense to define:

$$K_{f,natural} \equiv \left(1 - \gamma^2\right) \frac{1}{2\tau} m\epsilon^2 \tag{21}$$

... where ϵ^2 results from a term of vertical velocity over horizontal velocity, $\frac{1}{2}m$ is due to a kinetic energy term, τ is the simplest natural period, and $\left(1 - \gamma^2\right)$ is a term that tries to account for energy losses at each impact. By construction, we expect $K_{f,natural}$ to approximate K_f during resonant modes. Being that the actual value for this prediction involved the effective mass of the tip for energy conversion, and that this effective mass is essentially a fit to the model, no specific value for $K_{f,natural}$ will be listed here.

VII. NUMERICAL OBSERVATIONS DUE TO DIRECT SIMULATION

Performing direct simulations of this model allows observation of how the predictions given by dimensional and qualitative arguments compare to the model in detail. Careful exploration of the system is rather difficult to do fully, due to a 5-dimensional phase space, two variable parameters γ and v_0, quasiperiodic structures, and the singular behavior of grazing orbits in impact dyanmics. However, we can address specific results within this attractor with the hope that future work may build on this paper.

First, the most practical result is a sketch of the friction coefficient in Figure 1. The overall form is as predicted from arguments about how K_f changes with η, with the scale set by a maximum (in computational units) of about 0.0001. Taking into account the rescaling of time into τ (not $\tau_{computational}$) and the ϵ^2 term in $K_{f,natural}$, we see the naturally rescaled K_f is reasonably near unity from these multiples.

The second set of results, being tests of scaling, affirm several predictions from the dimensional section above. Though the γ dependence in K_f was not tested thoroughly, the scaling of mean period between impact and vertical velocity qualitatively fit dimensional arguments. Mean times looked nearly periodic in 2η, with unnoticeable net increase with increasing η over several integers (ignoring small structure). For velocity scaling, this result was most easily seen for $\eta \approx 2$ by plots of trajectories in spatial coordinates being similar in vertical scale to the amplitude of the surface, and for higher η by the scaling of K_f depend in a predicted (consistent) manner. Plots of mean time are not included, since a short written description suffices for overall net behavior.

We would enjoy, ideally, a zoology of the attractors that can occur within this model. Such a task would be a serious undertaking, and was not done in this project. Of the attractors that have been seen: stable periodic

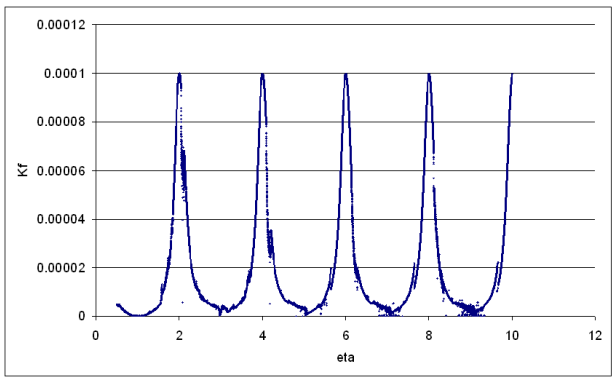

FIG. 1: Friction coefficient (with units mass=1, time=$\tau_{computational}$, and using $\gamma = 0.7$) vs. *eta*. The general behavior is as expected. There are some points at the higher η that look noisy near zero K_f, but this is a computational issue that should be averaged out "by eye" and not taken too seriously. Sampling information is not referenced here, but the plot is such that cutting sampling in half kept the graph visually similar within the order of thickness of the plot's line.

orbits, quasi-periodic orbits, chattering cascades (if we do not change the restitution coefficient for small impacts), and potentially chaotic orbits. Observed transitions between these include period doubling cascades, the so called grazing bifurcation [7], and others.

VIII. ATTEMPTED SYMBOLIC DYNAMICS

At this point of the project, the state of the symboic dynamics remains mostly a mystery. The richness of the system, coupled to the fact that phase space is 5-dimensional, defies an intuitive understanding, which we can get in 3 or even 4-dimensional phase space. We can never see more than a projection of the Poincare map's attractor. Attempts were made to use unstable manifolds to help partition phase space, but the typically complex expanding eigenvalues on periodic orbits did not open themselves readily to this treatment.

The one easily attainable periodic structure was periodic orbits, most often found quickly from rough guesses through a variational method. When found, these periodic orbits often reflect well the overall flow of the system. Figures 2 and 3 are plots of a particular attractor and its first periodic orbit. We should not be surprised, given the rough shadowing of the periodic orbit onto the attractor, that the periodic orbit gets the friction within 6 percent error - an already nice approximation.

The reassuring agreement in this orbit prompted a search for period two orbits, the results of which reflect some of the frustration inherent in this project. I found approximate bounds for the attractor and performed a 4-dimensional scan on the Poincare map. Two distinct regions appeared, and were subsequently run into periodic orbit search routines. One of the resulting regions contained, sensibly, the short periodic orbit that we already knew, repeated twice.

The other region contained a "false" periodic orbit that would not converge under Newton root finding nor resolve within accuracy a periodic orbit under the variational approach. We would expect, and we found numerically this to be true, that this false orbit would become a true periodic orbit by changing parameters slightly. Still, we cannot be honest and include this orbit in periodic orbit expansions for the given attractor.

Hence, we expect from this investigation that length 2 prime orbits have all been pruned for these particular parameters. Pruning so quickly is disheartening, and the hope of finding simple symbolic dyanmics is lessened. Possibly toying with generating/adapting partitions could predict prime orbits effectively, but this has yet to be done.

IX. SPECULATED FUTURE DIRECTION

Though we can arrive at plots of various expectation values to an accuracy well within the limits to test general structure and to compare roughly with experiment, knowing the symbolic dyanmics remains a conceptually inviting problem. With symbolic dyanmics known, the underlying structure of the billiard flow is better understood, and we could potentially begin to generate observ-

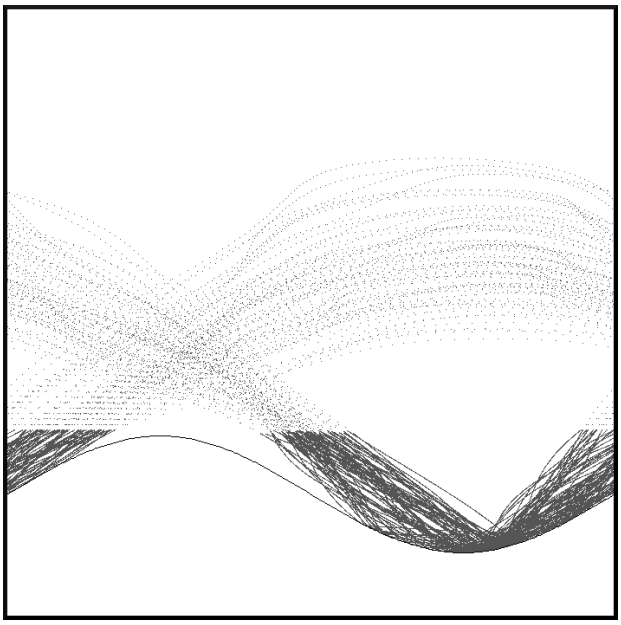

FIG. 2: The spatial projection of an attractor for $\gamma = 0.7$, $\eta = 3.4$. The sinusoid on the bottom is the surface, while the rest is (in scaled space) the AFM tip's trajectory. The sparse dots on the top are merely due to plotting, and should be considered comparably dense to the rest of the plot.

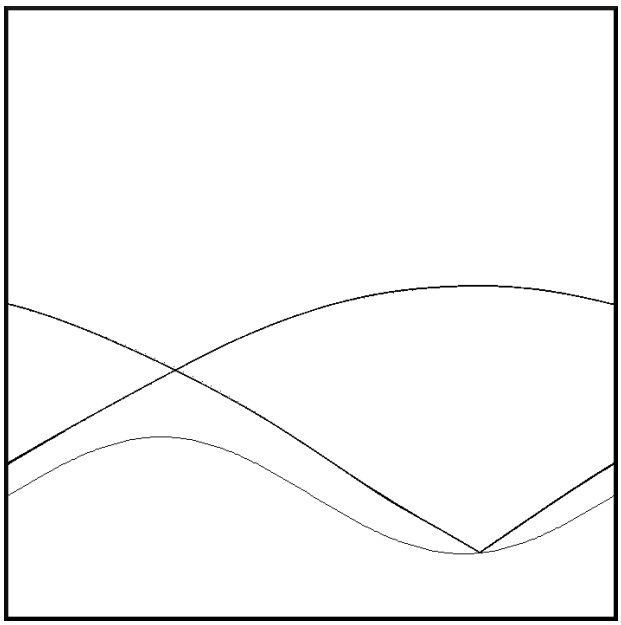

FIG. 3: The spatial projection of the periodic orbit found for $\gamma = 0.7$, $\eta = 3.4$.

ables to high accuracy. We say "potentially", because the presence of quasi-periodic unstable structures are not included in cycle expansions at this point in time, which could leave a measureable error in expectation values.

A simpler model can be derived from the present model, with reduced dimensions likely simplifying all the problems found for the present model. Thinking that the high horizontal frequency keeps the horizontal stretching small, we might surpress the horizontal stretching entirely and have an oscillating "hammer" bouncing across a periodic surface. This model is close to the impact oscillators found in the literature, partially referenced in the introduction of this paper. The overall dimension would be 3, and the Poincare map would have dimension 2. Thus, Smale horseshoe ideas should work well.

Most likely, further development of this model will be directly related to experimental observations supporting or denying predictions. In case of supporting evidence, the above recommendations might give good description of dyanmical frictional behavior.

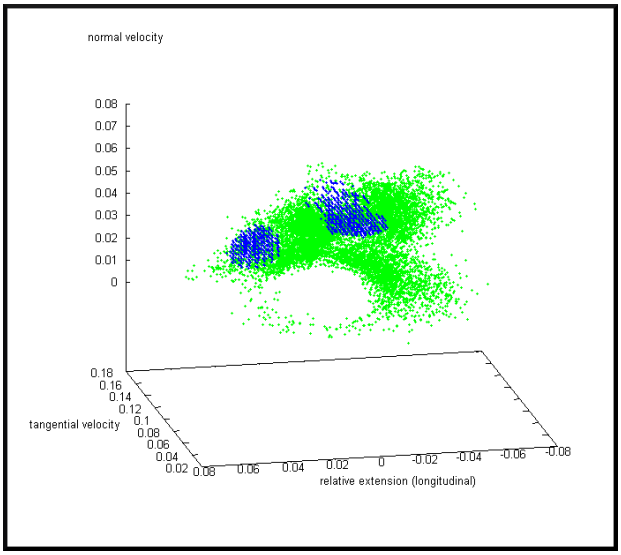

FIG. 4: Projection of a scan for period 2 orbits for $\gamma = 0.7$, $\eta = 3.4$. Points with lower norm (most likely to contain periodic structures) are colored dark blue (or just dark).

[1] P. Gaspard, *Chaos, scattering, and statistical mechanics* (Cambridge University Press, 1998).

[2] Binnig G, Quate CF, Gerber C. "Atomic Force Microscope," *Phys Rev Lett* **56**, 930-933 (1986).

[3] Gyalog T, Thomas H. "Atomic Friction," *Z. Phys. B* **104**, 669674 (1997).

[4] P. Cvitanović *et al.*, *Chaos: Classical and Quantum*, advanced graduate e-textbook, available online at `ChaosBook.org` (Niels Bohr Institute, Copenhagen 2005).

[5] Sasaki N, Fujisawa S, Sugawara Y, *et al.*, "Theoretical analysis of atomic-scale friction in frictional-force microscopy," *Abstr Pap Am Chem S* **213**, 59-COLL Part 1, (1997).

[6] Luck JM, Mehta A. "Bouncing Ball with a Finite Restitution: Chattering, Locking, and Chaos," *Phys. Rev. E* **48**, 3988-3997 (1993).

[7] Chin W, Ott E *et al.* "Grazing Bifurcations in Impact Oscillators," *Phys. Rev. E* **50**, 4427-4444 (1994).

[8] Weger J, Binks D *et al.* "Generic Behavior of Grazing Impact Oscillators." *Phys. Rev. Lett.* **76**, 3951-3954 (1996).

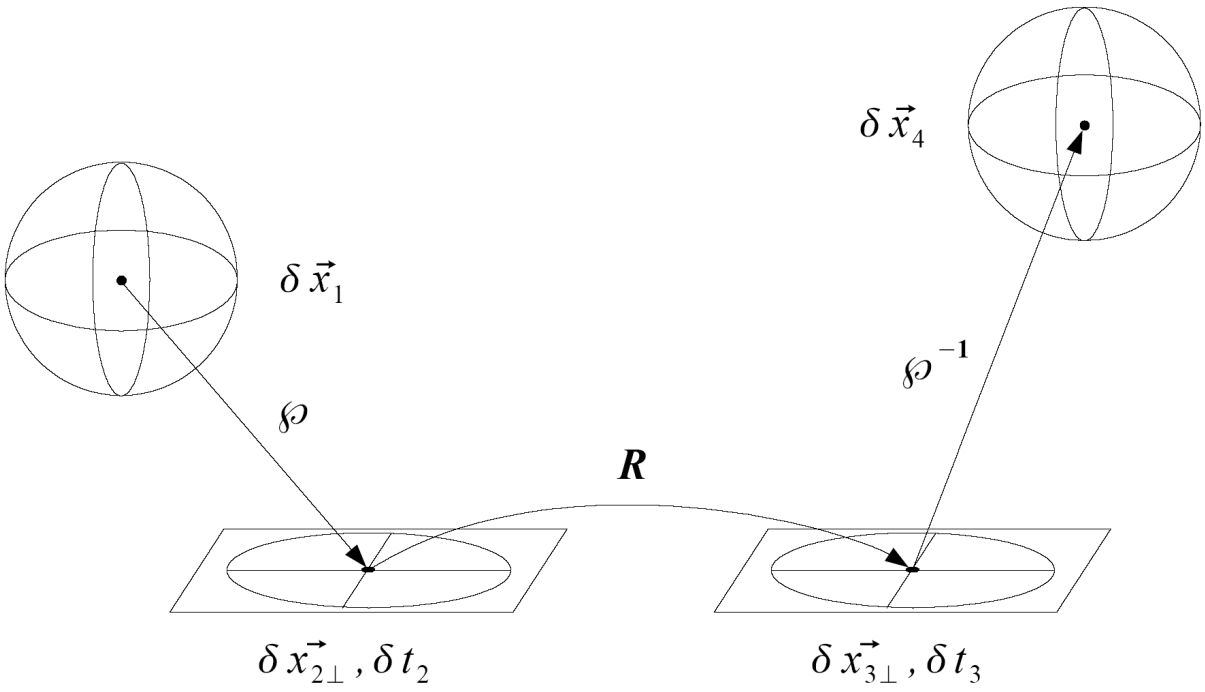

FIG. 5: Diagram for neighborhood calculation for Jacobians with mixed flows and maps. Refer to text.